Schizosaccharomyces pombe Calmodulin, Cam1, Plays a Crucial Role in Sporulation by Recruiting and Stabilizing the Spindle Pole Body Components Responsible for Assembly of the Forespore Membrane[∇][†]

Akiko Itadani,[1] Taro Nakamura,[1] Aiko Hirata,[2] and Chikashi Shimoda[1]*

Department of Biology, Graduate School of Science, Osaka City University, Sugimoto, Sumiyoshi-ku, Osaka 558-8585, Japan,[1] and Bioimaging Center, Graduate School of Frontier Sciences, University of Tokyo, Kashiwa, Chiba 277-8562, Japan[2]

Calmodulin in *Schizosaccharomyces pombe* is encoded by the *cam1*⁺ gene, which is indispensable for both vegetative growth and sporulation. Here, we report how Cam1 functions in spore formation. We found that Cam1 preferentially localized to the spindle pole body (SPB) during meiosis and sporulation. Formation of the forespore membrane, a precursor of the plasma membrane in spores, was blocked in a missense *cam1* mutant, which was viable but unable to sporulate. Three SPB proteins necessary for the onset of forespore membrane formation, Spo2, Spo13, and Spo15, were unable to localize to the SPB in the *cam1* mutant although five core SPB components that were tested were present. Recruitment of Spo2 and Spo13 is known to require the presence of Spo15 in the SPB. Notably, Spo15 was unstable in the *cam1* mutant, and as a result, SPB localization of Spo2 and Spo13 was lost. Overexpression of Spo15 partially alleviated the sporulation defect in the *cam1* mutant. These results indicate that calmodulin plays an essential role in forespore membrane formation by stably maintaining Spo15, and thus Spo2 and Spo13, at the SPB in meiotic cells.

Calmodulin is a calcium-binding protein that is ubiquitously distributed and highly conserved among eukaryotes. It contains four EF-hand Ca^{2+}-binding sites, which are required for function. Calmodulin controls a variety of cellular processes mostly related to calcium signaling. When bound to calcium, calmodulin undergoes a characteristic conformational change to an active configuration. Activated calmodulin then binds effector proteins and transmits the signal to downstream regulators.

Yeast is a genetically tractable model organism suitable for studying the biological function of calmodulin, using conditional-lethal calmodulin mutants (4). In the budding yeast *Saccharomyces cerevisiae*, calmodulin is encoded by the *CMD1* gene (5). Cmd1p is implicated in a wide variety of cellular processes, including initiation of budding and mitotic spindle formation (24). The fission yeast *Schizosaccharomyces pombe* has a typical calmodulin encoded by the *cam1*⁺ gene, which plays an indispensable role in cell proliferation, dependent on its Ca^{2+}-binding activity (18, 19, 30). A green fluorescent protein (GFP)-Cam1 fusion protein localizes to sites of polarized cell growth and to the spindle pole body (SPB) in vegetative cells (19). Thus, an essential role of Cam1 might be its regulatory function in chromosome segregation (19). The role of calmodulin in the sexual cycle has been documented to a lesser extent in previous studies. A missense mutant, *cam1-117*, in which the Arg117 codon is changed to a Phe codon, exhibits reduced

sporulation efficacy (29), suggesting that calmodulin plays a role in sporulation in fission yeast.

Spore formation in fission yeast initiates with assembly of the forespore membrane (FSM), composed of double-unit membranes within the cytoplasm of a diploid zygote cell (10, 27, 28, 34). The FSM expands to encapsulate each haploid nucleus generated by meiosis and then forms a nucleated prespore. The inner bilayer of the FSM subsequently becomes the plasma membrane of the newborn spores. During meiosis II, the SPB undergoes morphological alteration from a compact single plaque to a multilayered expanded structure (10). Such modification of the SPB is a prerequisite for FSM assembly, which occurs close to the outermost layer of the modified SPB (9, 10, 20, 21).

Three SPB component proteins, Spo2, Spo13, and Spo15, have been identified as essential for SPB modification and formation of the FSM (11, 23). Spo15, a large coiled-coil protein, is associated with the SPB throughout the life cycle and is indispensable for recruitment of Spo2 and Spo13 to the cytoplasmic surface of the meiotic SPB. The latter two proteins are produced only during meiosis (23). These observations imply that the SPB serves as a platform for assembly of the FSM. Cam1 has been reported to localize to the SPB during vegetative growth (19), raising the intriguing possibility that fission yeast calmodulin is involved in sporulation through proper construction of a modified meiotic SPB. To test this possibility, we report herein a detailed analysis of Cam1 localization during meiosis and the consequence of a missense mutation of *cam1* on SPB modification and FSM formation.

MATERIALS AND METHODS

Yeast strains, media, and culture conditions. The *S. pombe* strains used in this study are listed in Table 1. The complete medium YEA (yeast extract agar) was

---

* Corresponding author. Mailing address: Department of Biology, Graduate School of Science, Osaka City University, Sugimoto, Sumiyoshi-ku, Osaka 558-8585, Japan. Phone and fax: 81 66605 2576. E-mail: shimoda@sci.osaka-cu.ac.jp.

TABLE 1. *S. pombe* strains used in this study

Strain (accession no.)[a]	Genotype[b]	Source or reference
AI22 (FY19908)	h^{90} cam1-22,117≪ura4$^+$ ura4-D18 leu1-32	This study
AI52 (FY19909)	h^{90} cam1-22,117≪ura4$^+$ ura4-D18 ade6≪gfp-psy1	This study
AI154 (FY19910)	h^{90} spo15-gfp≪LEU2 leu1-32	This study
AI156 (FY19911)	h^{90} cam1-22,117≪ura4$^+$ ura4-D18 spo15-GFP≪LEU2 leu1-32	This study
AI190 (FY19912)	h^{90} cam1-22,117≪ura4$^+$ ura4-D18 sid4-gfp::Kn^r leu1-32	This study
AI197 (FY19913)	h^{90} cam1-22,117≪ura4$^+$ ura4-D18 cut12-gfp::ura4$^+$	This study
AI200 (FY19914)	h^{90} cut12-gfp≪ura4$^+$ ura4-D18	This study
AI207 (FY19915)	h^{90} cam1-22,117≪ura4$^+$ ura4-D18 alp4-gfp::Kn^r	This study
AI210 (FY19916)	h^{90} spo15::ura4$^+$ade6≪gfp-cam1 ura4-D18	This study
AI248 (FY19917)	h^{90} ade6≪gfp-cam1	This study
AI258 (FY19918)	h^{90} leu1≪spo13-gfp	This study
AI259 (FY19919)	h^{90} leu1≪spo2-gfp	This study
AI262 (FY19920)	h^{90} cam1-22,117≪ura4$^+$ ura4-D18 leu1≪spo2-gfp	This study
AI263 (FY19921)	h^{90} cam1-22,117≪ura4$^+$ ura4-D18 leu1≪spo13-gfp	This study
AI350 (FY19922)	h^{90} cam1-22,117≪ura4$^+$ ura4-D18 leu1≪pcp1-gfp	This study
AI351 (FY19923)	h^{90} leu1≪pcp1-gfp	This study
AI509 (FY19924)	h^{90}/h^{90} cam1::ura4$^+$/cam1$^+$ ade6-M210/ade6-M216 leu1-32/leu1-32 ura4-D18/ura4-D18	This study
AI510 (FY19925)	h^{90} cam1::ura4$^+$ leu1≪cam1$^+$ ura4-D18 leu1-32 ade6-M216	This study
AI512 (FY19926)	h^{90} cam1::ura4$^+$ leu1≪cam1-22 ura4-D18 leu1-32 ade6-M216	This study
AI518 (FY19927)	h^{90} cam1::ura4$^+$ leu1≪cam1-22,117 ura4-D18 leu1-32 ade6-M216	This study
AI520 (FY19928)	h^{90} cam1::ura4$^+$ leu1≪cam1-EF1 ura4-D18 leu1-32 ade6-M216	This study
AI522 (FY19929)	h^{90} cam1::ura4$^+$ leu1≪cam1-EF2 ura4-D18 leu1-32 ade6-M216	This study
AI524 (FY19930)	h^{90} cam1::ura4$^+$ leu1≪cam1-EF3 ura4-D18 leu1-32 ade6-M216	This study
AI526 (FY19931)	h^{90} cam1::ura4$^+$ leu1≪cam1-EF4 ura4-D18 leu1-32 ade6-M216	This study
AI16 (FY12806)	h^{90} ura4-D18 ade6-M210 leu1-32	A. Itadani
AI2030 (FY19932)	h^{90} leu1≪gfp-cam1$^+$ ura4-D18 ade6-M210 leu1-32	This study
AI2031 (FY19933)	h^{90} leu1≪gfp-cam1-22,117 ura4-D18 ade6-M210 leu1-32	This study
AI2032 (FY19934)	h^{90} leu1≪gfp-cam1-22 ura4-D18 ade6-M210 leu1-32	This study
AI2033 (FY19935)	h^{90} leu1≪gfp-cam1-EF1 ura4-D18 ade6-M210 leu1-32	This study
AI2034 (FY19936)	h^{90} leu1≪gfp-cam1-EF2 ura4-D18 ade6-M210 leu1-32	This study
AI2035 (FY19937)	h^{90} leu1≪gfp-cam1-EF3 ura4-D18 ade6-M210 leu1-32	This study
AI2036 (FY19938)	h^{90} leu1≪gfp-cam1-EF4 ura4-D18 ade6-M210 leu1-32	This study
AI3001 (FY19939)	h^{90} cam1::ura4$^+$ leu1≪cam1-22 ura4-D18 leu1-32 ade6-M216 [pREP1(ade6)]	This study
AI3002 (FY19940)	h^{90} cam1::ura4$^+$ leu1≪cam1-22 ura4-D18 leu1-32 ade6-M216 [pREP1(ade6)cam1$^+$]	This study
AI3003 (FY19941)	h^{90} cam1::ura4$^+$ leu1≪cam1-22 ura4-D18 leu1-32 ade6-M216 [pREP1(ade6)cam1-22]	This study
AI3004 (FY19942)	h^{90} cam1::ura4$^+$ leu1≪cam1-22,117 ura4-D18 leu1-32 ade6-M216 [pREP1(ade6)]	This study
AI3005 (FY19943)	h^{90} cam1::ura4$^+$ leu1≪cam1-22,117 ura4-D18 leu1-32 ade6-M216 [pREP1(ade6)cam1$^+$]	This study
AI3006 (FY19944)	h^{90} cam1::ura4$^+$ leu1≪cam1-22,117 ura4-D18 leu1-32 ade6-M216 [pREP1(ade6)cam1-22,117]	This study
AI3007 (FY19945)	h^{90} cam1::ura4$^+$ leu1≪cam1-EF2 ura4-D18 leu1-32 ade6-M216 [pREP1(ade6)]	This study
AI3008 (FY19946)	h^{90} cam1::ura4$^+$ leu1≪cam1-EF2 ura4-D18 leu1-32 ade6-M216 [pREP1(ade6)cam1$^+$]	This study
AI3009 (FY19947)	h^{90} cam1::ura4$^+$ leu1≪cam1-EF2 ura4-D18 leu1-32 ade6-M216 [pREP1(ade6)cam1-EF2]	This study
AI3010 (FY19948)	h^{90} cam1::ura4$^+$ leu1≪cam1-EF3 ura4-D18 leu1-32 ade6-M216 [pREP1(ade6)]	This study
AI3011 (FY19949)	h^{90} cam1::ura4$^+$ leu1≪cam1-EF3 ura4-D18 leu1-32 ade6-M216 [pREP1(ade6)cam1$^+$]	This study
AI3012 (FY19950)	h^{90} cam1::ura4$^+$ leu1≪cam1-EF3 ura4-D18 leu1-32 ade6-M216 [pREP1(ade6)cam1-EF3]	This study
MFP7 (FY19951)	h^- gfp::cam1 ade1-D25 ade6-M210 leu1-32 ura4-D18	19
S60-3 (FY12208)	h^{90} sid4-gfp::Kn^r leu1-32	K. Okazaki
TN8 (FY7132)	h^{90} leu1-32	20
YN24 (FY12250)	h^{90} ade6-M210	Y. Nakase
YM20 (FY12096)	h^{90} ade6≪gfp-psy1	14
YN104 (FY12332)	h^{90} spo15::ura4$^+$ leu1-32 ade6-M210 ura4-D18	23
YN372 (FY12550)	h^{90} alp4-gfp::Kn^r leu1-32	Y. Nakase

[a] Accession numbers are from the Yeast Genetic Resource Center of Japan supported by the National BioResource Project (YGRC/NBRP; http:/yeast.lab.nig.ac .jp/nig/). The *S. pombe* strains constructed in this study have been deposited with the YGRC/NBRP under the accession numbers shown here.
[b] $x ≪ y$ means that gene y is integrated at gene x.

used for growth. Malt extract agar (MEA) medium and synthetic sporulation media (MM-N and SSA) were used for mating and sporulation. These media have been described in Moreno et al. (17). *S. pombe* cells were grown and sporulated at 28°C.

Plasmid construction. The plasmids used in this study are listed in Table 2. The *cam1$^+$* gene was cloned into the pAL-KS vector as described below. The *cam1$^+$* gene was amplified by PCR using 5′-GCAGCCTCGAG(XhoI)AGAAT AAACTATATAAAATCTTTAAA-3′ and 5′-GAGCTAAATAATGGGCATGGG AATTGCAAG-3′ as forward and reverse primers, respectively. The PCR product was digested with XhoI and SpeI and then ligated into the corresponding sites of pAL-KS to yield pAL(cam1). The 2.4-kb ApaI-SacI fragment of the pAL(cam1) was inserted into pBR322 to yield pBR(cam1).

The *gfp-cam1$^+$* fusion gene was constructed and integrated at the *cam1* locus (19). The *gfp-cam1$^+$* fusion gene was amplified by PCR using genomic DNA from the MPF7 strain and the PCR primers 5′-GCAGCCTCGAG (XhoI)AGA ATAAACTATAAAATCTTTAAA-3′ (forward) and 5′-GAGCTAAATAATG GGCATGGGAATTGCAAG-3′ (reverse). A 3.0-kb ApaI-SacI fragment was inserted into pAL-KS to yield pAL(GFP-cam1). Plasmid pIA(GFP-cam1) was constructed by inserting the same fragment from pAL(GFP-cam1) into the pIA integration vector (K. Tamai, personal communication).

Western blotting. The abundance of Spo15 in vegetative and meiotic cells was evaluated by Western blotting with anti-Spo15 antibody. The abundance of GFP-Cam1 in cells was analyzed by Western blotting using anti-GFP antibody. The pIA(GFP-cam1) plasmid carrying the *cam1* promoter and a coding region

TABLE 2. Plasmids used in this study

Plasmid	Description	Source or reference
pAL-KS	*ars1 LEU2*-based vector	31
pBR(leu1)	*leu1*[+] in pBR322	22
pREP1	*ars1 LEU*[+]-based vector carrying a thiamine-repressible *nmt1* promoter	16
pIL2	*LEU2*-based integration vector	20
pIA	*ade6*[+]-based integration vector	K. Tamai
pAL(cam1)	*cam1*[+] in pAL-KS	This study
pAL(gfp-cam1)	*gfp-cam1*[+] in pAL-KS	This study
pIA(gfp-cam1)	*gfp-cam1*[+] in pIA1	This study
pREP1(ade6)	*ade6*[+]-based expression vector	T. Nakamura
pREP1(ade6)gfp-cam1[+]	*gfp-cam1*[+] in pREP1(ade6)	This study
pREP1(ade6)gfp-cam1-22	*gfp-cam1-22* in pREP1(ade6)	This study
pREP1(ade6)gfp-cam1-22,117	*gfp-cam1-22,117* in pREP1(ade6)	This study
pREP1(ade6)gfp-cam1-EF2	*gfp-cam1-EF2* in pREP1(ade6)	This study
pREP1(ade6)gfp-cam1-EF3	*gfp-cam1-EF3* in pREP1(ade6)	This study
pBR322(spo13-gfp)	*spo13*[+]-gfp in pBR(leu1)	Y. Nakase
pBR322(spo2-gfp)	*spo2*[+]-gfp in pBR(leu1)	Y. Nakase
pREP1(spo2)	*spo2*[+] in pREP1	Y. Nakase
pREP1(spo13)	*spo13*[+] in pREP1	Y. Nakase
pREP1(spo15)	*spo15*[+] in pREP1	T. Nakamura
pIA(gfp-psy1)	*gfp-psy1*[+] in pIA	14
pBR(gfp-cam1[+])	*gfp-cam1*[+] in pBR(leu1)	This study
pBR(cam1[+])	*cam1*[+] in pBR(leu1)	This study
pBR(cam1-22)	*cam1-22* in pBR(leu1)	This study
pBR(cam1-22,117)	*cam1-22,117* in pBR(leu1)	This study
pBR(cam1-EF1)	*cam1-EF1* in pBR(leu1)	This study
pBR(cam1-EF2)	*cam1-EF2* in pBR(leu1)	This study
pBR(cam1-EF3)	*cam1-EF3* in pBR(leu1)	This study
pBR(cam1-EF4)	*cam1-EF4* in pBR(leu1)	This study

for GFP-Cam1 was linearized by restricting it with BamHI near the center of the *ade6*[+] sequence and then introduced into an *ade6* strain (YN24 and YN104). The resulting *gfp-cam1* integrant strains, AI248 and AI210, were cultured in MM-N sporulation medium. At intervals, portions of the culture were sampled, and crude cell extracts were prepared as described by Masai et al. (15). Polypeptides were resolved by SDS-polyacrylamide gel electrophoresis on 7.5% gels (for Spo15) or 10% gels (for GFP-Cam1) and then transferred onto polyvinylidene difluoride membranes (Millipore, Bedford, MA). Membranes were probed with anti-Spo15 antibody (23) at a 1:100 dilution or with mouse anti-GFP antibody (Roche, Basel, Switzerland) at a 1:200 dilution. Blots were also probed with anti-α-tubulin antibody, TAT1 (32), to normalize protein loading. Immunoreactive bands were visualized by chemiluminescence (NEN Life Sciences, Boston, MA) using horseradish peroxidase-conjugated goat anti-mouse IgG (GE Healthcare, Little Chalfont, Buckinghamshire, United Kingdom).

Fluorescence microscopy. The SPB was visualized by immunofluorescence microscopy. Cells were fixed with glutaraldehyde and paraformaldehyde (8). The SPB was visualized by using rabbit anti-Sad1 antibody (a gift from O. Niwa, Kazusa DNA Research Institute) and Alexa Fluor 546- or 488-conjugated secondary antibody (Molecular Probes, Eugene, OR). Sad1 is a major SPB component required for bipolar spindle formation (7). The nuclear chromatin region was stained with 4′,6′-diamidino-2-phenylindole (DAPI) at 1 μg/ml or Hoechst 33342 at 1 μg/ml (Nakarai Tesque, Kyoto, Japan). Stained cells were observed under a fluorescence microscope (model BX50; Olympus, Tokyo, Japan). To assess SPB modification quantitatively, stained cells were observed under a fluorescence microscope (model IX-71; Olympus), and SPB width was measured by AQUACOSMOS software (Hamamatsu Photonics, Shizuoka, Japan).

The FSM was observed by GFP-Psy1 fluorescence imaging (20). Psy1 is a plasma membrane-resident t-SNARE protein that is homologous to budding yeast Sso1 and Sso2 (1) and human syntaxin-1 (2). The *gfp-psy1* fusion gene was integrated at the *ade6* locus on chromosome III (14).

Electron microscopy. Samples for electron microscopy were prepared as described previously (33), and sections were viewed on an electron microscope (H-7600; Hitachi, Tokyo, Japan) at 100 kV.

Mutants of Cam1 Ca^{2+}-binding sites. Cam1 contains four EF-hand Ca^{2+}-binding sites (18). Each of the four EF-hand motifs was mutated by replacing a conserved glutamic acid residue with valine. The wild-type *cam1*[+] gene cloned in

an integration vector, pBR(leu1), was subjected to site-directed mutagenesis. A commercial *in vitro* mutagenesis kit was used (QuikChange; Stratagene, La Jolla, CA). The *cam1* mutant allele in EF-hand binding site 1 was designated *cam1-EF1*. The other alleles were designated similarly. Each of the mutant genes (*cam1-EF1*, *cam1-EF2*, *cam1-EF3*, and *cam1-EF4*) was integrated at the *leu1*[+] locus in a heterozygous *cam1*[+]/*cam1*::*ura4*[+] diploid strain (AI509). The integrant strains were sporulated to isolate meiotic segregants carrying the *cam1* point mutation in the *cam1*::*ura4*[+] background. The resulting strains were AI510 (*cam1*[+]), AI520 (*cam1-EF1*), AI522 (*cam1-EF2*), AI524 (*cam1-EF3*), and AI526 (*cam1-EF4*) (Table 1). The *cam1-22* and *cam1-22,117* alleles were created by the same method (AI512 and AI518).

GFP-tagged *cam1* mutant genes were constructed in an integration vector carrying *leu1*[+] as a selectable marker. The *gfp-cam1* fusion gene was expressed under the authentic *cam1* promoter. Plasmid pBR(gfp-cam1[+]) was then subjected to site-directed mutagenesis as mentioned above (QuikChange; Stratagene, La Jolla, CA). In this way, modified pBR(leu1) plasmids containing either *gfp-cam1-22,117*, *gfp-cam1-22*, *gfp-cam1-EF1*, *gfp-cam1-EF2*, *gfp-cam1-EF3*, or *gfp-cam1-EF4* were created. These plasmids were linearized by digestion with Eco81I and then used to transform the AI16 strain (h^{90} *leu1-32 cam1*[+]). The plasmids were integrated at the *leu1* locus by homologous recombination to create strains AI2030 to AI2036 (Table 1).

In order to overproduce the Cam1 proteins, the *gfp*-tagged *cam1* genes in plasmid pBR(gfp-cam1[+]) were recloned into expression vector pREP1(ade6) (Table 2). The constructed plasmids carrying the *gfp*-tagged *cam1* missense mutant genes were subsequently introduced into the respective *cam1* mutant strains (Table 1, AI3001 to AI3012).

Deposition and accession numbers of strains. The *S. pombe* strains constructed in this study have been deposited with the YGRC/NBRP under accession numbers FY19908 to FY19951.

RESULTS

GFP-Cam1 localizes to the SPB during meiosis. In vegetative cells, GFP-Cam1, which has previously been shown to be functional (19), localizes to both the polarized cell sur-
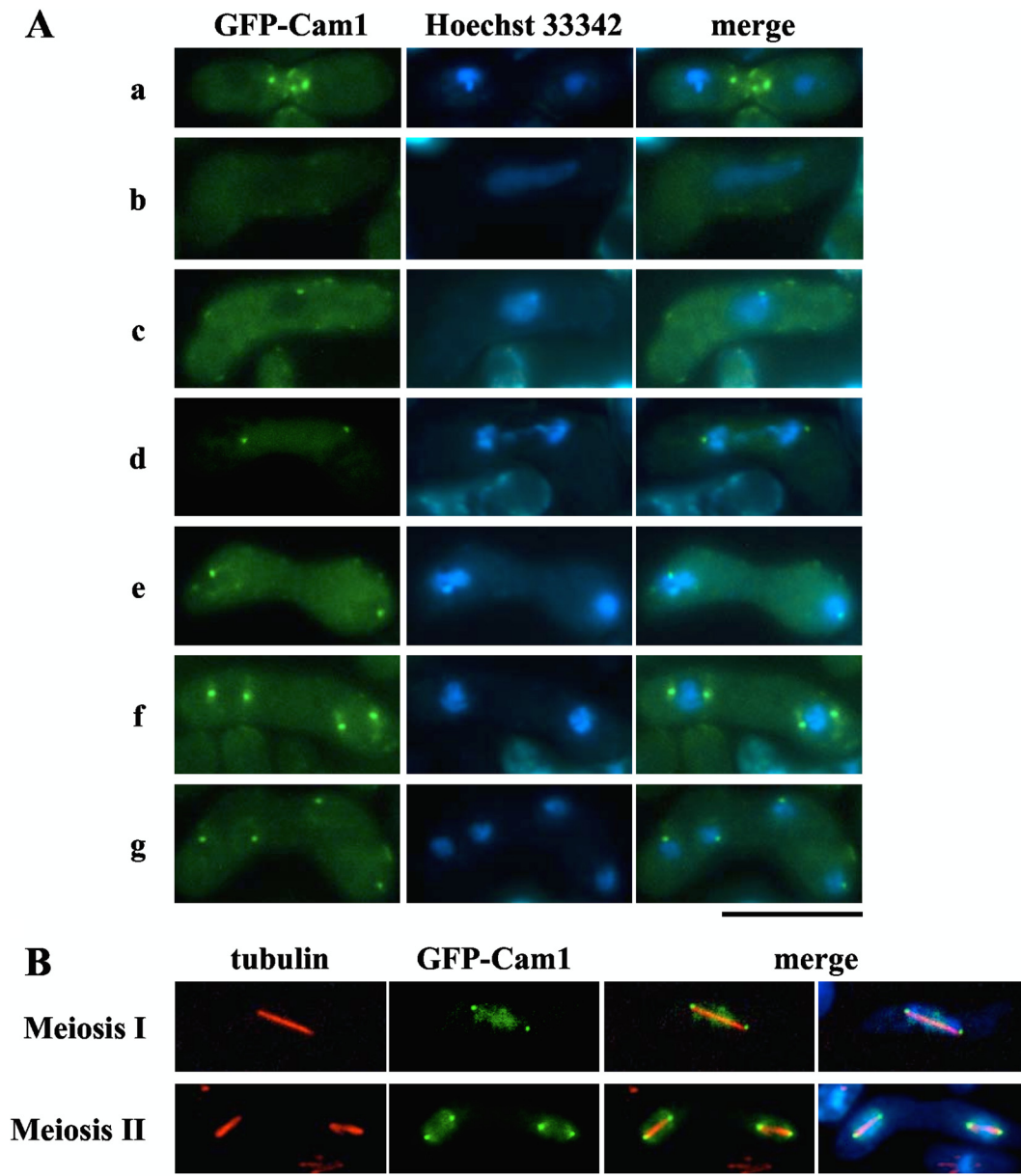
FIG. 1. Cellular localization of Cam1 during mating, meiosis, and sporulation. The homothallic haploid strain AI248 harboring a *gfp-cam1* fusion gene was cultured on SSA medium to induce the sexual cycle. (A) Cells were stained with Hoechst 33342 to visualize nuclei. Developmental stages shown are as follows: row a, before karyogamy; row b, horsetail stage; row c, before meiosis I; row d, meiosis I; row e, interphase; row f, early meiosis II; row g, after meiosis II. Bar, 10 μm. (B) Cells were fixed during meiosis. Microtubules and nuclei were visualized by anti α-tubulin antibody, TAT1 (red) (32), and DAPI (blue), respectively. Bar, 10 μm.

face at growing tips and the SPB (19). Here, we analyzed localization of GFP-Cam1 during the sexual cycle (Fig. 1), induced by shifting haploid cells to a nitrogen-limiting sporulation medium. After induction, the GFP-Cam1 signal in the SPB and cell poles disappeared, while the fluorescent signal was subsequently detected as several bright patches at the site of cell fusion between cells of opposite mating types (Fig. 1A, row a). After nuclear fusion, meiosis ensues in a diploid zygote. In meiotic prophase I, the nucleus with an elongated shape moves actively back and forth (a so-called horsetail nucleus) (3). Here, the punctate GFP-Cam1 sig-

nals disappeared as cells entered the horsetail stage (Fig. 1A, row b). Intense signals appeared again as dots near the nuclear periphery soon after prophase I (Fig. 1A, row c). These dots duplicated in parallel with meiotic divisions (Fig. 1A, rows d to g), suggesting that Cam1 accumulates at the SPB as in vegetative cells. To test this idea, cells expressing GFP-Cam1 were fixed and immunostained with anti-α-tubulin antibody, TAT1 (32). As shown in Fig. 1B, GFP-Cam1 dots were positioned at both ends of the meiotic spindles. Localization of GFP-Cam1 to the SPB was also confirmed by double staining with anti-Sad1 antibody (data not
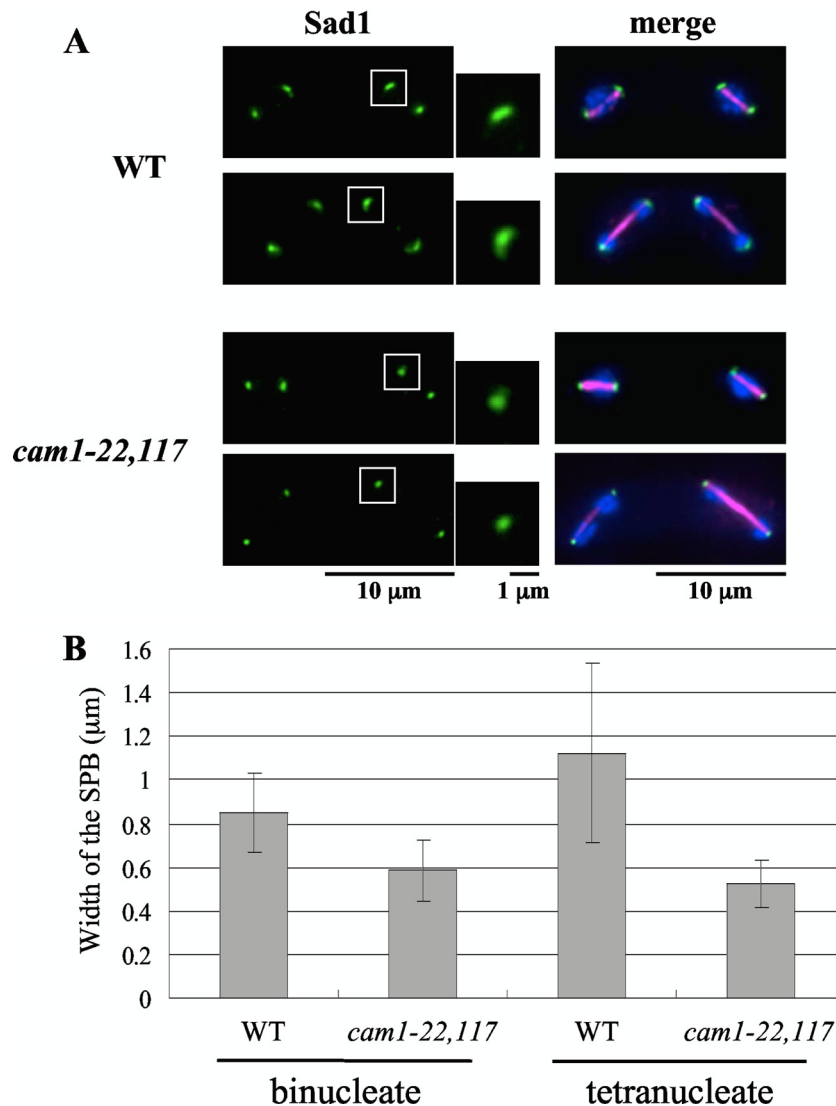
FIG. 2. Structural modification of the SPB during sporulation. The TN8 (h^{90} $cam1^+$) and AI22 (h^{90} $cam1$-$22,117$) strains were cultured on MEA sporulation medium. (A) Immunostaining of the SPB with anti-Sad1 antibody (green). Magnified images of the boxed regions are also presented. Meiotic stages of the cells were examined by staining nuclei with DAPI (blue) and spindle microtubules with anti-α-tubulin antibody, TAT1 (magenta). (B) Comparison of the width of the SPB between wild-type and $cam1$-$22,117$ strains. Binucleate and tetranucleate cells were determined separately. The means $\pm$ standard deviations of approximately 100 SPBs are shown.

shown). Sad1 is an SPB protein necessary for bipolar spindle formation (7).

$cam1$ missense mutants fail to form the FSM. Because $cam1^+$ is essential for growth, the $cam1$ disruptant is inviable. Thus, the role of Cam1 in sporulation was assessed by using viable missense mutants. The missense mutant allele $cam1$-$22,117$ harbors two mutations, D22Y (in which Asp22 is replaced by Tyr) and R117F (in which Arg117 is replaced by Phe). This haploid mutant exhibited no growth defects, but homozygous diploids failed to sporulate. The $cam1$-$22,117$ mutant was isolated spontaneously from descendants of the $cam1$-117 mutant generated by Takeda et al. (29) based on exhibiting a strict Spo$^-$ phenotype. The sporulation defect of the $cam1$-$22,117$ strain was suppressed by introducing plasmid pAL-KS harboring $cam1^+$ (see Figure 7).

Because the processes of meiosis and spore formation in S.

$pombe$ are closely related, we first tested the kinetics of meiosis in the $cam1$-$22,117$ mutant. There was no significant difference between the wild-type and $cam1$-$22,117$ mutant cultures (data not shown). Sporulation itself proceeds through three steps: (i) structural change in the SPB (SPB modification), (ii) FSM assembly, and (iii) spore wall formation (27). Prior to spore formation, the SPB undergoes a characteristic alteration, as revealed by electron and fluorescence microscopy (7, 10). Our previous studies indicated that SPB modification was essential for initiation of FSM assembly (11, 23). To study defects in sporulation in detail, we first explored structural changes in the SPB during meiosis II, as revealed by immunofluorescence microscopy. The SPB in wild-type cells changes morphology from a compact dot to a crescent form, but such a structural change was not marked in the $cam1$-$22,117$ mutant (Fig. 2A). Poor development of the SPB in
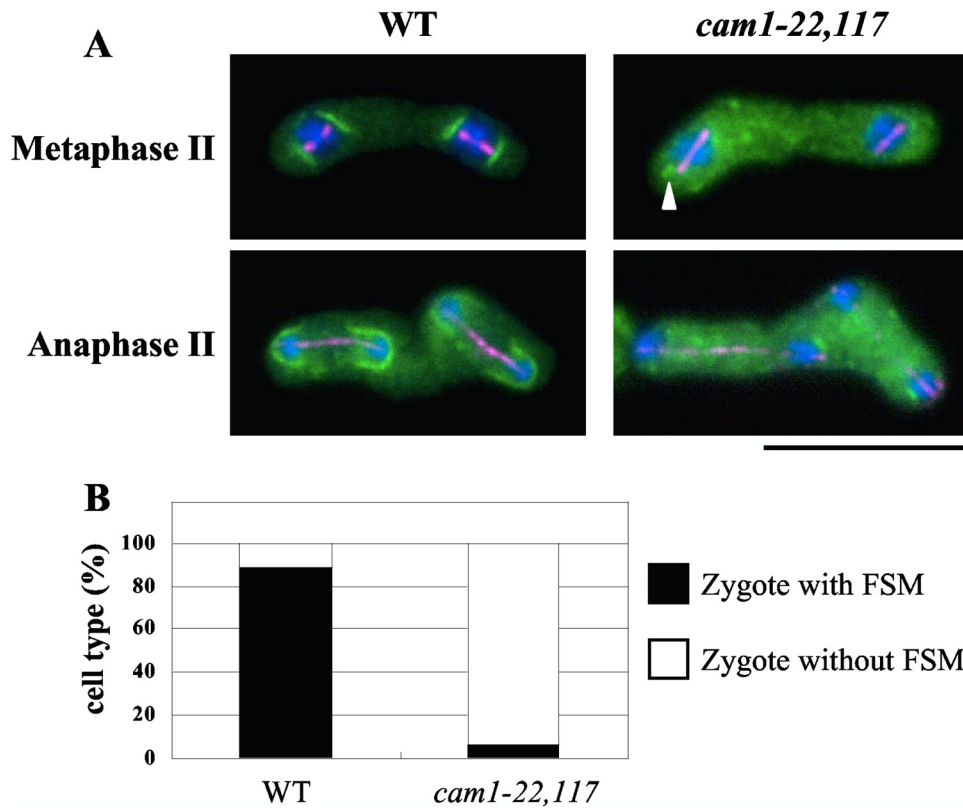
FIG. 3. Initiation of FSM assembly in the *cam1-22,117* mutant. (A) The nascent FSM was visualized by GFP-psy1 (green). A *cam1+* strain (YM20) and a *cam1-22,117* strain (AI52) were cultured on MEA sporulation medium and doubly stained with anti-α-tubulin antibody, TAT1 (magenta), and DAPI (blue). The arrowhead indicates a very short FSM-like structure. Bar, 10 μm. (B) Quantitative assay for zygote formation with an FSM. Only zygotes that assembled meiosis II spindles were counted.

the *cam1* mutant was confirmed quantitatively by measuring the width of the SPB (Fig. 2B).

Next, we monitored FSM formation by using GFP-Psy1. Psy1 localizes to the plasma membrane of mother cells in meiosis I and then accumulates in the nascent FSM in meiosis II (14, 20). The FSM was observed as bright lines or arcs near both ends of the spindles of wild-type zygotes at early meiosis II and then extended as the spindles elongated (Fig. 3A). In the *cam1-22,117* mutant, cup-shaped GFP-Psy1 signals were barely seen at the termini of short and long spindles. Instead, dots or very short lines of GFP-Psy1 were discernible near the nuclei in some cells. The percentage of zygotes forming any FSM-like structures in the *cam1* mutant was only 5%, in contrast to 90% observed in the wild-type strain (Fig. 3B).

To examine SPB morphology and the FSM-like structures in *cam1-22,117* zygotes, the fine structure was observed by electron microscopy. As shown in Fig. 4, the outer plaques of the SPB in the *cam1-22,117* mutant were poorly developed. Furthermore, the FSM initiated in some cells, but even in such cells its expansion was severely inhibited. We conclude that FSM formation is blocked at an early stage in the *cam1-22,117* mutant.

Spo2, Spo13, and Spo15 cannot localize to the SPB in the *cam1-22,117* mutant. We reported earlier that the coiled-coil protein Spo15 is a constitutive SPB component required for sporulation but dispensable for vegetative growth (11). Two other sporulation-specific SPB components, Spo2 and Spo13,

are recruited to the SPB in a Spo15-dependent manner during meiosis (23). Localization of Spo13 to the meiotic SPB relies on Spo2, which physically interacts with both Spo13 and Spo15. Proper recruitment of Spo13 is necessary for construction of the outer plaques on which the FSM is initially assembled. The above results show that Cam1 also localizes to the SPB during meiosis (Fig. 1) and is essential for SPB modification (Fig. 2). We therefore tested whether the sporulation-related SPB components, Spo2, Spo13, and Spo15, localize to the SPB in the *cam1-22,117* mutant (Fig. 5).

In vegetative cells expressing Spo15-GFP, the fluorescent signal localized to the SPB in a wild-type strain (Fig. 5A) as previously reported (11). Notably, the signal was not restricted to the SPB but was diffuse throughout the cytoplasm in vegetative *cam1-22,117* cells (Fig. 5B), indicating that the SPB localization of Spo15 requires Cam1 function. Furthermore, the intensity of the Spo15-GFP fluorescence markedly decreased in meiotic cells (Fig. 5B). Spo2-GFP and Spo13-GFP signals did not localize to the SPB but were dispersed in the nucleus in the *cam1-22,117* mutant. These observations are consistent with our previous finding that Spo2 and Spo13 in the *spo15* deletion strain exhibited nuclear localization (23).

Because the *cam1-22,117* mutation impaired localization of SPB components required only for spore formation, we next examined localization of other SPB components essential for growth, namely, Sad1, Cut12, Alp4, Sid4, and Pcp1, a conserved calmodulin target protein closely related to *S. cerevisiae*
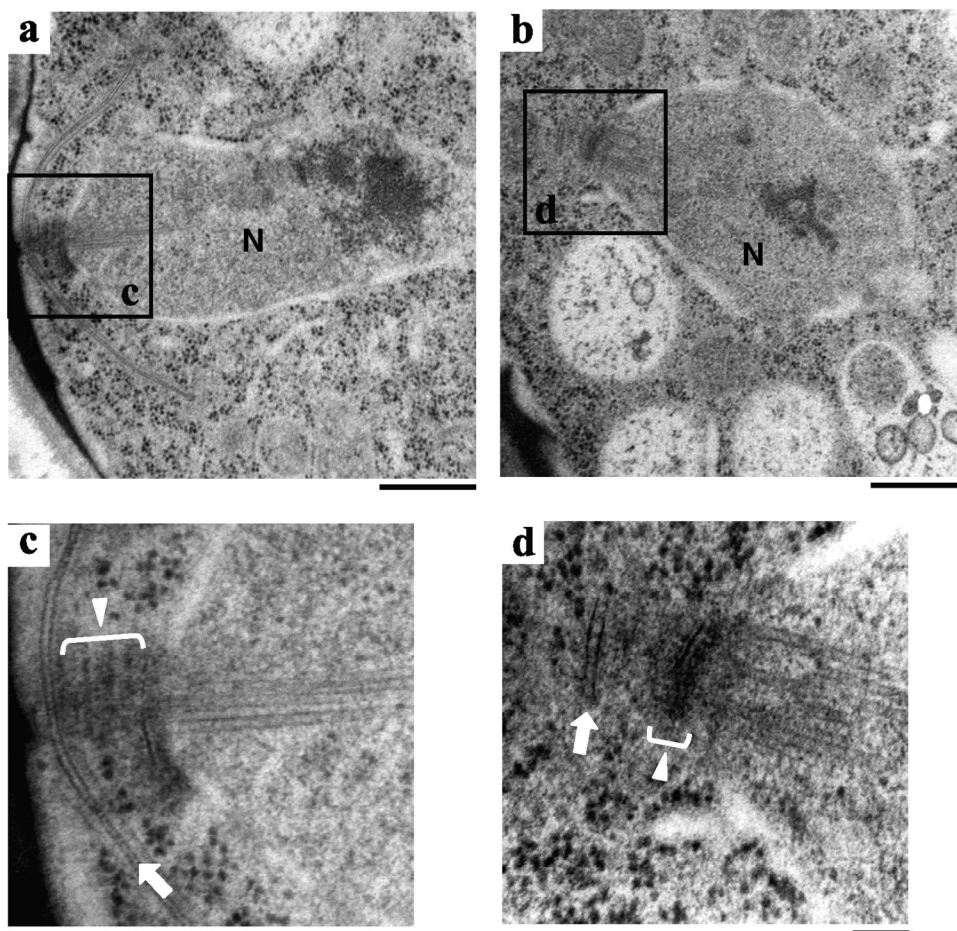
FIG. 4. Fine structures of wild-type and *cam1-22,117* strains during meiosis II. Cells were fixed after incubation on MEA sporulation medium for 1 day. Electron microscopic images of the wild-type (a and c) and *cam1-22,117* (b and d) strains. Panels c and d are magnified images of the boxed regions in panels a and b, respectively. N, nucleus; white lines with triangles, the SPB; white arrows, the expanding FSM (c) and the abortive FSM (d). Bars, 500 nm (a and b) and 100 nm (c and d).

Spc110 (6). These proteins localized to the SPB both in the wild-type and the *cam1-22,117* strains (see Fig. S1 in the supplemental material). As far as we tested, only sporulation-related SPB components were affected by the *cam1* mutation.

We asked whether GFP-Cam1 could localize to the SPB in a *spo15Δ* mutant in sporulation medium. GFP-Cam1 was observed at the SPB as in wild-type cells (see Fig. S2 in the supplemental material). Nearly the same results were obtained with *spo2Δ* and *spo13Δ* (data not shown). These observations suggest that Cam1 localization to the SPB does not depend on Spo15, Spo2, or Spo13 but, rather, that Cam1 governs normal recruitment of these proteins to the SPB.

Spo15 is unstable in the *cam1-22,117* mutant. As shown in Fig. 5B, the Spo15-GFP signal was less intense in the *cam1-22,117* mutant than in the wild-type strain during meiosis. To verify this observation, the level of Spo15 protein during vegetative growth and sporulation was assayed by Western blotting using an anti-Spo15 antibody. We also examined the effect of the single *cam1-22* mutation. The AI510 (*cam1+*), AI 512 (*cam1-22*), and AI518 (*cam1-22,117*) strains were incubated in growth medium for 20 h and then transferred to and incubated in sporulation medium for 8 h. Spo15 protein levels in vege-

tative cells were roughly the same in these three strains (Fig. 6A). In sporulating cells, however, the *cam1-22,117* and *cam1-22* mutations severely reduced Spo15 protein levels (Fig. 6A). These results imply that Cam1 is needed to stabilize the Spo15 protein under sporulation conditions. Abundance of the Cam1 protein was then examined in the *spo15Δ* strain. GFP-Cam1 abundance was not affected by the *spo15* deletion in sporulating cells (Fig. 6B).

Overexpression of Spo15 partially alleviates the sporulation defect in the *cam1-22,117* mutant. The aforementioned results suggested that the sporulation defect in *cam1-22,117* is due to a reduction in Spo15 abundance. We therefore tested whether overexpression of Spo15 might alleviate the sporulation defect in the *cam1-22,117* mutant. As shown in Fig. 7, overexpression of Spo15 slightly but significantly enhanced ascus formation in the mutant, whereas overexpression of Spo13 or Spo2 did not. These results suggest that Cam1 is involved in sporulation, at least in part through maintenance of sufficient levels of Spo15.

Other mutations at Cam1 Ca²⁺-binding sites also affect sporulation. The *cam1-22,117* mutant harbors two mutations at Asp22 and Arg117. Asp22 is one of the acidic residues in the EF-hand Ca^{2+}-binding site 1. Because Cam1 has four EF-hand
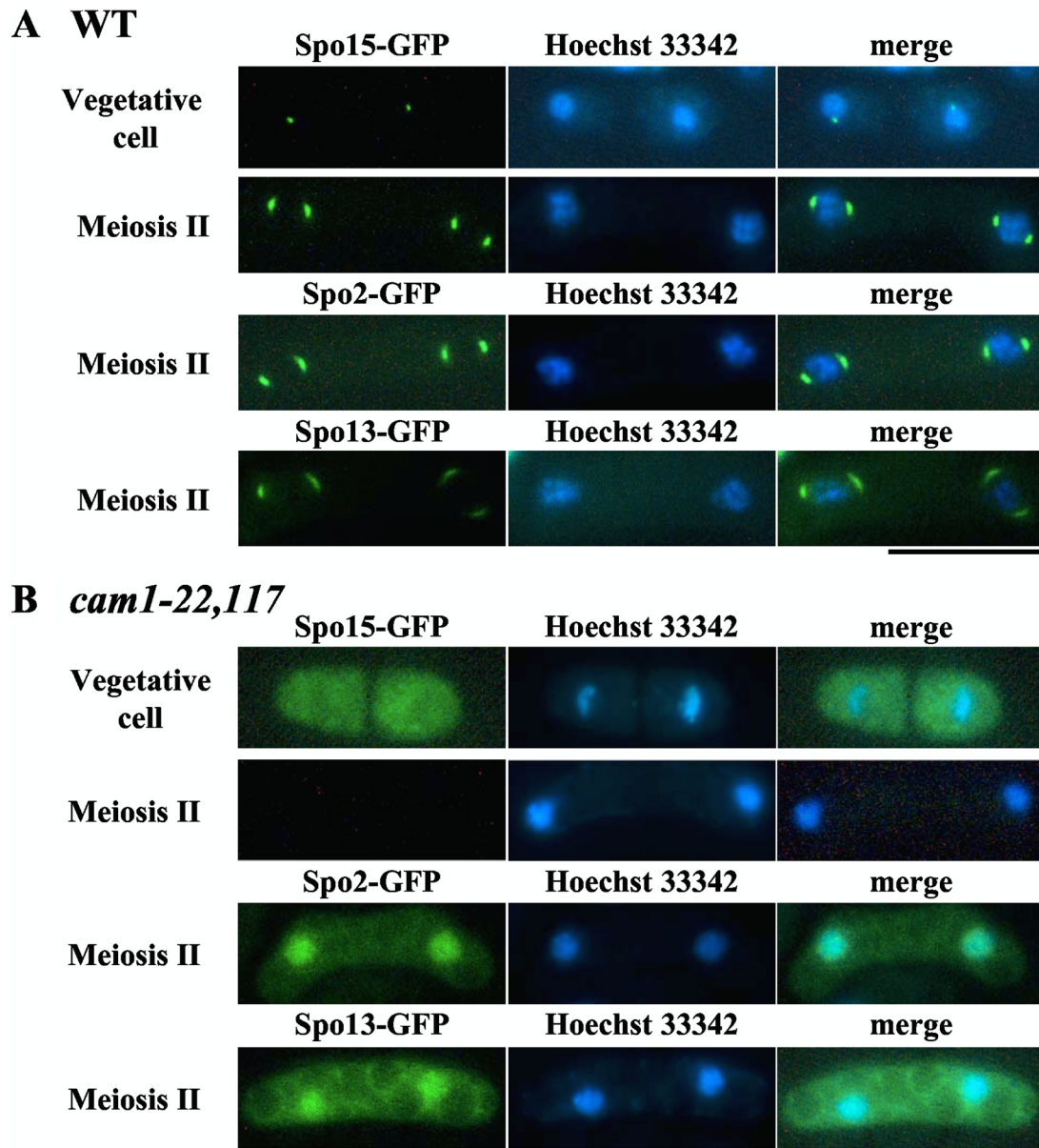
A WT

B cam1-22,117

FIG. 5. Localization of Spo15, Spo2, and Spo13 in wild-type and *cam1-22,117* strains. (A) Homothallic wild-type (*cam1⁺*) strains expressing Spo15-GFP (AI154), Spo2-GFP (AI259), or Spo13-GFP (AI258) were cultured on complete (YEA) and sporulation (SSA) media. Cells were stained with Hoechst 33342 (blue). Bar, 10 μm. (B) Similarly, homothallic *cam1-22,117* strains, expressing Spo15-GFP (AI156), Spo2-GFP (AI262), or Spo13-GFP (AI263), were cultured on YEA and SSA media. Bar, 10 μm.

motifs, we tested whether Ca^{2+}-binding site mutants exhibited a sporulation defect. The conserved Glu residue in each of the four EF-hand motifs was replaced with Val. The *cam1-EF1*, *cam1-EF2*, *cam1-EF3*, and *cam1-EF4* mutants harbor E33V, E69V, E106V, and E142V substitutions, respectively (18).

We found that the *cam1-22* mutant was unable to sporulate although another *cam1-EF1* mutant (*cam1-E33V*) sporulated normally (Fig. 8) as did the *cam1-EF4* mutant. In contrast, the *cam1-EF2* mutant harboring a missense mutation at the second binding site exhibited a severe sporulation defect, while the *cam1-EF3* mutant exhibited a moderate defect. These results suggest that the first, second, and third Ca^{2+}-binding sites of calmodulin play important roles in spore formation.

Stability of the mutant Cam1 protein under sporulation conditions. Takeda et al. (29) reported that the Cam1-117 protein was unstable under nitrogen starvation conditions. It is probable that the defects in spore formation in different *cam1* mutants observed here were due to decreased stability of Cam1 in sporulation cultures. To test this possibility, levels of the mutant Cam1 proteins that were tagged with GFP were analyzed by Western blotting. As shown in Fig. S3 in the supplemental material, the quantity of all the mutant proteins was roughly the same as wild-type Cam1 during incubation in sporulation medium. These results suggest that inability of *cam1* mutants to complete spore formation is not due to reduced abundance of Cam1. To confirm this conclusion, we
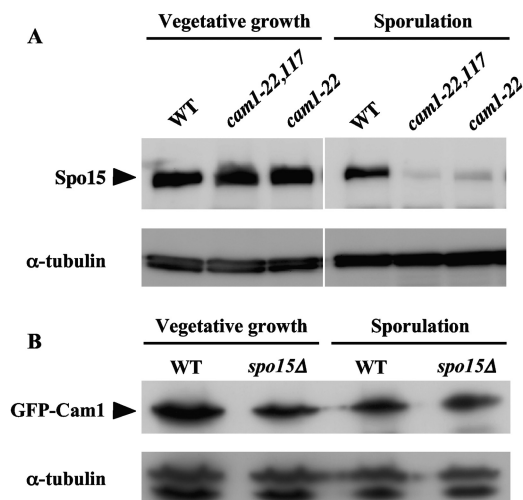
FIG. 6. Detection of Spo15 and Cam1 by Western blotting. (A) Western analysis of Spo15. Strains AI510 (*cam1*[+]), AI512 (*cam1-22*), and AI518 (*cam1-22,117*) were cultured in liquid synthetic medium, MM+N, for 20 h (vegetative growth) and liquid sporulation medium, MM-N, for 8 h (sporulation). Protein extracts were subjected to immunoblotting with anti-Spo15 antibody and with anti-α-tubulin antibody as a loading control. (B) Western analysis of Cam1. AI248 (*cam1*[+]) and AI210 (*spo15Δ*) strains expressing GFP-Cam1 were cultured in MM+N for 8 h and in MM-N for 6 h. Protein extracts were subjected to immunoblotting with anti-GFP antibody and with anti-α-tubulin antibody as a loading control. WT, wild type.

tested whether overexpression of the mutant *cam1* gene would alleviate sporulation deficiency. As shown in Fig. S4 in the supplemental material, overexpression of mutant Cam1 did not affect sporulation efficiency. The lack of spore formation in these *cam1* missense mutants was not due to lability of the mutated Cam1 proteins, except for Cam1-117 (29), but could be due to defective structural features.

DISCUSSION

S. pombe has a typical calmodulin, Cam1, and a calmodulin-like protein, Cam2. Cam1 is essential for proliferation although Cam2 is dispensable for growth (12, 13, 28). Cam2 is a regulatory light chain of type I myosin (13). We previously reported that Cam2 localizes to the leading edge of the FSM and plays a role in sporulation at supraoptimum temperatures (12). In the present study, we report the molecular details of an indispensable role for *S. pombe* calmodulin Cam1 in spore formation. To determine the biological roles of calmodulin in fission yeast, we undertook a phenotypic analysis of *cam1* missense mutants focusing on sporulation processes. We made the following observations: (i) Cam1 preferentially localized to the SPB during meiosis and spore formation; (ii) SPB modification and proper FSM assembly required functional Cam1; (iii) a key SPB component, Spo15, which is necessary for sporulation, was mislocalized and unstable in *cam1* mutants; (iv) in addition to Spo15, two other SPB proteins necessary for spore formation, Spo2 and Spo13, failed to localize to the SPB in the *cam1* mutant. Taken together, these observations indicate that Cam1 modulates construction of the meiotic SPB that is a prerequisite for FSM assembly.

Cam1 is a constitutive component of the SPB and is necessary for bipolar spindle formation during mitosis (19). In *S. pombe*, another EF-hand-containing SPB protein is known, referred to as Cdc31, which is an ortholog of a conserved protein centrin (25, 26). Cdc31/centrin in yeasts is essential for SPB duplication (25). As shown in the present study, Cam1 is implicated in meiotic SPB modification required for FSM assembly. To our knowledge, there are no experimental data suggesting that *S. pombe* Cdc31 is also responsible for spore formation. The question of whether two EF-hand proteins, Cam1 and Cdc31, share a role in structural modification of the meiotic SPB to facilitate spore formation in *S. pombe* remains to be answered.

In vegetative cells, Cam1 interacts with Pcp1, a conserved calmodulin-binding SPB protein (6). Pcp1 overexpression failed to suppress the sporulation defect in the *cam1* mutant (data not shown). It is possible that Cam1 might interact with an additional effector protein in both mitotic and meiotic cells. One candidate protein is Spo15. This protein has features similar to Pcp1 in that it is a high-molecular-weight, coiled-coil SPB protein. Spo15 does not localize to the SPB (Fig. 5) and is unstable in the *cam1-22,117* mutant (Fig. 6). Overexpression of Spo15 in the *cam1* mutant partially alleviated the sporulation defect. These observations suggest that Cam1 interacts directly or indirectly with Spo15. However, we could not demonstrate a physical interaction between Cam1 and Spo15 by immunoprecipitation or the yeast two-hybrid assay (data not shown). A direct sporulation-related target for Cam1 remains to be elucidated.

S. pombe calmodulin Cam1 has four conserved EF-hand Ca^{2+}-binding sites (18). Conserved acidic residues in the EF-hand motif are important for Ca^{2+}-binding activities. Replacing these acidic residues with Val disrupts Ca^{2+}-binding capacity. A systematic mutagenesis experiment previously demonstrated that at least one of the four binding sites is needed for proliferation (18). Single disruptions of any four EF-hand motifs did not result in growth defects. In contrast, disruption of a specific EF-hand motif, e.g., EF2, caused a sporulation defect, suggesting that dependency of sporulation on Ca^{2+}-binding activity of EF-hand sites might be more specific. Quantitative Ca^{2+}-binding assay and phenotypic analysis indicated that binding site 2 is the most important for the essential mitotic function of Cam1 (18). Consistent with this result, our sporulation assay indicated that a single mutation in Ca^{2+}-binding site 2 caused a sporulation defect.

The single mutation in Ca^{2+}-binding site 1, *cam1-22* (D22Y), also conferred a sporulation-deficient phenotype. Surprisingly, replacement of the conserved Glu33 residue in binding site 1 with Val (*cam1-E1*) did not result in a loss of sporulation. Thus, replacing the two acidic residues, Asp22 and Glu33, with Val has different phenotypic consequences which could reflect the Ca^{2+}-free configurations of these mutant Cam1 proteins.

In summary, fission yeast calmodulin Cam1 plays an indispensable role in the SPB modification essential for FSM assembly. Cam1 stably maintains Spo15 at the SPB, which in turn recruits the other SPB component, Spo2, during meiosis. Finally, Spo13 accumulates at the outer layers of the meiotic SPB by physical interaction with Spo2. Spo13 plays a major role in the initial stage of FSM formation. Fission yeast calmodulin is

A

vector   pREP1 (spo15)

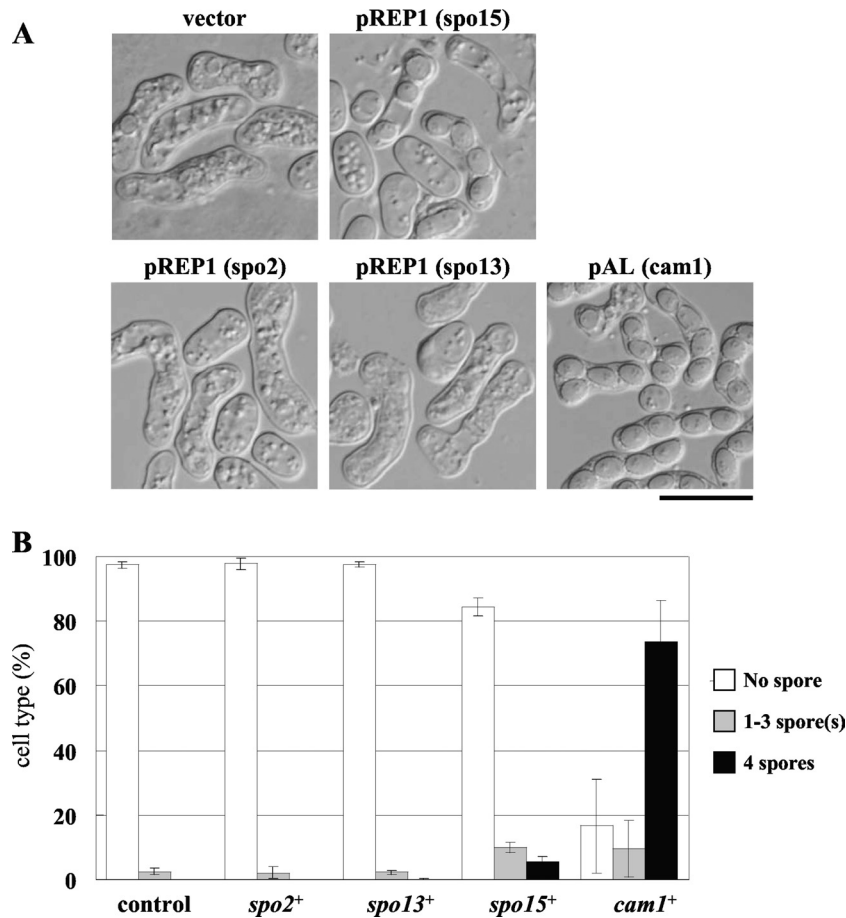pREP1 (spo2)   pREP1 (spo13)   pAL (cam1)

B

FIG. 7. Overexpression of Spo15, Spo2, and Spo13 in the *cam1-22,117* mutant. (A) The AI22 (*cam1-22,117*) strain was transformed with a pREP1 expression vector carrying *spo15+ spo2+* or *spo13+* and a multicopy plasmid carrying *cam1+*, pAL(cam1). Transformants were cultured on sporulation medium (SSA) for 2 days. Bar, 10 μm. (B) Sporulation was monitored by determining the percentage of asci, which were further classified according to the number of spores per ascus.

implicated in this ordered recruitment of three sporulation-specific SPB proteins. To our knowledge, this study provides the first insight into calmodulin function in sexual development in yeast.
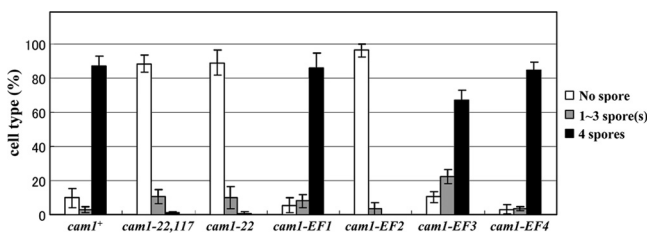

FIG. 8. Sporulation ability of the *cam1* mutant harboring mutations in EF-hand motifs. The wild-type *cam1+* and respective *cam1* mutant genes were integrated at the *leu1* locus on chromosome II of AI509. Strains used were AI510 (*cam1+*), AI512 (*cam1-22*), AI518 (*cam1-22, 117*), AI520 (*cam1-EF1*), AI522 (*cam1-EF2*), AI524 (*cam1-EF3*), and AI526 (*cam1-EF4*). Strains were cultured on MEA medium for 2 days, and their sporulation efficiencies were measured. The percentage of asci, classified according to the number of spores per ascus, is presented.

REFERENCES

1. **Aalto, M. K., H. Ronne, and S. Keränen.** 1993. Yeast syntaxins Sso1p and Sso2p belong to a family of related membrane proteins that function in vesicular transport. EMBO J. **12:**4095–4104.
2. **Bennett, M. K., N. Calakos, and R. H. Scheller.** 1992. Syntaxin: a synaptic protein implicated in docking of synaptic vesicles at presynaptic active zones. Science **257:**255–259.
3. **Chikashige, Y., D. Q. Ding, H. Funabiki, S. Mashiko, M. Yanagida, and Y. Hiraoka.** 1994. Telomere-led premeiotic chromosome movement in fission yeast. Science **264:**270–273.
4. **Cyert, M. S.** 2001. Genetic analysis of calmodulin and its targets in *Saccharomyces cerevisiae*. Annu. Rev. Genet. **35:**647–672.
5. **Davis, T. N., M. S. Urdea, F. R. Masiarz, and J. Thorner.** 1986. Isolation of the yeast calmodulin gene: calmodulin is an essential protein. Cell **47:**423–431.
6. **Flory, M. R., M. Morphew, J. D. Joseph, A. R. Means, and T. N. Davis.** 2002.

Pcp1p, an Spc110p-related calmodulin target at the centrosome of the fission yeast *Schizosaccharomyces pombe*. Cell Growth Differ. **13:**47–58.

7. **Hagan, I., and M. Yanagida.** 1995. The product of the spindle formation gene *sad1*+ associates with the fission yeast spindle pole body and is essential for viability. J. Cell Biol. **129:**1033–1047.

8. **Hagan, I. M., and J. S. Hyams.** 1988. The use of cell division cycle mutants to investigate the control of microtubule distribution in the fission yeast *Schizosaccharomyces pombe*. J. Cell Sci. **89:**343–357.

9. **Hirata, A., and C. Shimoda.** 1994. Structural modification of spindle pole bodies during meiosis II is essential for the normal formation of ascospores in *Schizosaccharomyces pombe*: ultrastructural analysis of *spo* mutants. Yeast **10:**173–183.

10. **Hirata, A., and K. Tanaka.** 1982. Nuclear behavior during conjugation and meiosis in the fission yeast *Schizosaccharomyces pombe*. J. Gen. Appl. Microbiol. **28:**263–274.

11. **Ikemoto, S., T. Nakamura, M. Kubo, and C. Shimoda.** 2000. *S. pombe* sporulation-specific coiled-coil protein Spo15p is localized to the spindle pole body and essential for its modification. J. Cell Sci. **113:**545–554.

12. **Itadani, A., T. Nakamura, and C. Shimoda.** 2006. Localization of type I myosin and F-actin to the leading edge region of the forespore membrane in *Schizosaccharomyces pombe*. Cell Struct. Funct. **31:**181–195.

13. **Lord, M., and T. D. Pollard.** 2004. UCS protein Rng3p activates actin filament gliding by fission yeast myosin-II. J. Cell Biol. **167:**315–325.

14. **Maeda, Y., J. Kashiwazaki, C. Shimoda, and T. Nakamura.** 2009. The *Schizosaccharomyces pombe* syntaxin 1 homolog, Psy1, is essential in the development of the forespore membrane. Biosci. Biotechnol. Biochem. **73:**339–345.

15. **Masai, H., T. Miyake, and K. Arai.** 1995. *hsk*+, a *Schizosaccharomyces pombe* gene related to *Saccharomyces cerevisiae CDC7*, is required for chromosomal replication. EMBO J. **14:**3094–3104.

16. **Maundrell, K.** 1993. Thiamine-repressible expression vectors pREP and pRIP for fission yeast. Gene **123:**127–130.

17. **Moreno, S., A. Klar, and P. Nurse.** 1990. Molecular genetic analysis of fission yeast *Schizosaccharomyces pombe*. Methods Enzymol. **194:**795–823.

18. **Moser, M. J., S. M. Lee, R. E. Klevit, and T. N. Davis.** 1995. Ca²⁺ binding to calmodulin and its role in *Schizosaccharomyces pombe* as revealed by mutagenesis and NMR spectroscopy. J. Biol. Chem. **270:**20643–20652.

19. **Moser, M. J., M. R. Flory, and T. N. Davis.** 1997. Calmodulin localizes to the spindle pole body of *Schizosaccharomyces pombe* and performs an essential function in chromosome segregation. J. Cell Sci. **110:**1805–1812.

20. **Nakamura, T., M. Nakamura-Kubo, A. Hirata, and C. Shimoda.** 2001. The *Schizosaccharomyces pombe spo3*⁻ gene is required for assembly of the forespore membrane and genetically interacts with *psy1*+-encoding syntaxin-like protein. Mol. Biol. Cell **12:**3955–3972.

21. **Nakamura, T., H. Asakawa, Y. Nakase, J. Kashiwazaki, Y. Hiraoka, and C. Shimoda.** 2008. Live observation of forespore membrane formation in fission yeast. Mol. Biol. Cell **19:**3544–3553.

22. **Nakamura-Kubo, M., T. Nakamura, A. Hirata, and C. Shimoda.** 2003. The fission yeast *spo14*+ gene encoding a functional homologue of budding yeast Sec12 is required for the development of forespore membranes. Mol. Biol. Cell **14:**1109–1124.

23. **Nakase, Y., M. Nakamura-Kubo, Y. Ye, A. Hirata, C. Shimoda, and T. Nakamura.** 2008. Meiotic spindle pole body bodies acquire the ability to assemble the spore plasma membrane by sequential recruitment of sporulation-specific components in fission yeast. Mol. Biol. Cell **19:**2476–2487.

24. **Ohya, Y., and D. Botstein.** 1994. Diverse essential functions revealed by complementing yeast calmodulin mutants. Science **263:**963–966.

25. **Paoletti, B., N. Bordes, R. Haddad, C. L. Schwartz, F. Chang, and M. Bornens.** 2003. Fission yeast cdc31p is a component of the half-bridge and controls SPB duplication. Mol. Biol. Cell **14:**2793–2808.

26. **Rice, L. M., and D. A. Agard.** 2002. Centriole duplication: Centrin in on answers? Curr. Biol. **12:**R618–R619.

27. **Shimoda, C.** 2004. Forespore membrane assembly in yeast: coordinating SPBs and membrane trafficking. J. Cell Sci. **117:**389–396.

28. **Shimoda, C., and T. Nakamura.** 2003. Control of late meiosis and ascospore formation, 311–327. *In* R. Egel (ed.), Molecular biology of *Schizosaccharomyces pombe*. Springer, Berlin, Germany.

29. **Takeda, T., Y. Imai, and M. Yamamoto.** 1989. Substitution at position 116 of *Schizosaccharomyces pombe* calmodulin decreases its stability under nitrogen starvation and results in a sporulation-deficient phenotype. Proc. Natl. Acad. U. S. A. **86:**9737–9741.

30. **Takeda, T., and M. Yamamoto.** 1987. Analysis and in *vivo* disruption of the gene coding for calmodulin in *Schizosaccharomyces pombe*. Proc. Natl. Acad. Sci. U. S. A. **84:**3580–3584.

31. **Tanaka, K., T. Yonekawa, Y. Kawasaki, Y. Kai, K. Furuya, M. Iwasaki, H. Murakami, M. Yanagida, and H. Okayama.** 2000. Fission yeast Eso1p is required for establishing sister chromatid cohesion during S phase. Mol. Cell. Biol. **20:**3459–3469.

32. **Woods, A., T. Sherwin, R. Sasse, T. MacRae, A. J. Baines, and K. Gull.** 1989. Definition of individual components within the cytoskeleton of Trypanosoma brucei by a library of monoclonal antibodies. J. Cell Sci. **93:**491–500.

33. **Ye, Y., M. Fujii, A. Hirata, M. Kawamukai, C. Shimoda, and T. Nakamura.** 2007. Geranylgeranyl diphosphate synthase in fission yeast is a heteromer of farnesyl diphosphate synthase (FPS), Fps1 and an FPS-like protein, Spo9, essential for sporulation. Mol. Biol. Cell **18:**3568–3581.

34. **Yoo, B. Y., G. B. Calleja, and B. F. Johnson.** 1973. Ultrastructural changes of the fission yeast (*Schizosaccharomyces pombe*) during ascospore formation. Arch. Mikrobiol. **91:**1–10.